

Investigations on a Large Collection of Cosmic Dust From the Central Indian Ocean

Krishnakant Parashar · M. Shyam Prasad · S. S. S. Chauhan

Received: 21 October 2008 / Accepted: 13 September 2010 / Published online: 6 October 2010
© Springer Science+Business Media B.V. 2010

Abstract We collected 1,245 spherules from the Central Indian Ocean basin by Magnetic cosmic dust collection (MACDUC) experiment raking the deep sea floor. This collection ranks among the large deep sea collections of cosmic dust. For this study, 168 particles are analyzed with SEM-EDS to characterise their cosmic nature and identify the processes that their morphological features, textures and chemical compositions reveal. All the three basic types of cosmic spherules have been identified: I-type, S-type and the G-type. The silicate or the S-type spherules are dominant in this collection. In all, 115 spherules were sectioned, polished and analyzed for major elements. I-type spherules are mainly composed of Fe and Ni oxides, some have metallic cores where appreciable amounts of Co is observed in addition to glassy phases with lithophile elements are also observed in these spherules. These evidences are supportive of the view that the I-type spherules could be metal grains from carbonaceous/unequilibrated chondritic bodies. The S-type spherules show elemental composition of Mg, Al, Si, Ca, Fe, and Ni approximately similar to chondritic compositions. In addition, some other rare particles such as an S-type sphere which contains a large zoned relict chromite crystal, other spheres with a semi-porphyritic/barred olivine texture are also observed. While most the S-type spherules appear to have carbonaceous chondrites as their parent bodies, the relict grain bearing spherule shows distinctly an ordinary chondritic parent body.

Keywords Cosmic spherules · Cosmic dust · Micrometeorites · Chondrites · Carbonaceous chondrites · Central Indian Ocean

K. Parashar · M. S. Prasad (✉)
Geological Oceanography Division, National Institute of Oceanography,
Council for Scientific and Industrial Research, Dona Paula, Goa 403004, India
e-mail: shyam@nio.org

S. S. S. Chauhan
Karlsruhe Institute of Technology, Institut für Meteorologie und Klimaforschung,
Forschungszentrum Karlsruhe, Karlsruhe, Germany

1 Introduction

About 30,000 tonnes of cosmic dust of all sizes rains on the Earth annually (Love and Brownlee 1993; Peucker-Ehrenbrink 2001) which is mainly produced by the fragmentation of asteroids and released from comets, reaching Earth's surface in the form of millimeter sized particles called micrometeorites; some micrometeorites (<50 μm) survive atmospheric entry and reach the Earth unmelted (Flynn 1989; Love and Brownlee 1993) whereas others undergo partial to complete melting during their hypervelocity entry into the earth's atmosphere and are recoverable as dark coloured, spherical, solidified droplets called cosmic spherules (Millard and Finkleman 1970; Blanchard et al. 1980; Maurette et al. 1987; Taylor et al. 2000).

Cosmic spherules, for the first time, were retrieved from deep sea sediments during the HMS Challenger expedition (Murray and Renard 1883) where both stony and iron types were found and their origin was assigned to ablating meteoroids. Subsequently, cosmic spherules have been collected from diverse environments including beach sands (Marvin and Einaudi 1967), desert sands (Fredriksson and Gowdy 1963), lithified sedimentary formations (Czajkowski et al. 1983; Jehanno et al. 1988; Taylor and Brownlee 1991), Antarctica ice (Koeberl and Hagen 1989; Maurette et al. 1991; Taylor et al. 2000), from the Transantarctic Mountains (Rochette et al. 2008), Greenland blue water lakes (Maurette et al. 1986; Robin et al. 1990) and from glacial sediments of Novaya Zemlya archipelago, Russia (Badjukov and Raitala 2003). It is expected that majority of the cosmic dust particles are ferromagnetic in nature due to presence of magnetite which forms during atmospheric entry, and therefore, collection can be made employing simple techniques using hand held magnets. Although weathering alters the surface of particles, large numbers of cosmic dust have been collected from deep sea sediments using simple magnetic techniques (Millard and Finkleman 1970; Brownlee et al. 1979; Blanchard et al. 1980; Murrell et al. 1980) in view of the low sedimentation rates in these regions and the relatively easier accessibility as compared with the Polar Regions.

Earlier investigations (e.g. Ganapathy et al. 1983; Blanchard et al. 1980) provided proof of the extraterrestrial origin of cosmic spherules and established reasonably unambiguous criteria for the identification of three principal spherule class types namely I-type, S-type and G-type. Iron type spherules are smooth, shiny black and comprised of magnetite and wustite with or without FeNi bead. These spherules have their Fe, Ni, and Co ratios compatible with meteorites. Stony spherules comprising barred/zoned olivine and magnetite crystals with interstitial glass have major element compositions close to primitive solar system material such as CI, CM and CR chondrites (Kurat et al. 1994; Brownlee et al. 1997; Enggrand and Maurette 1998). G-type spherules consist of dendritic magnetite in silicate glass matrix with very high Fe content (Blanchard et al. 1980). Further, Taylor et al. (2000) investigated large numbers of micrometeorites from the Antarctica and defined the sequence of heating and melting of chondritic material which is reflected in the textures of S-type cosmic spherules. More recently, taking into consideration the results from all earlier investigations, Genge et al. (2008) gave a classification of micrometeorites. It has been suggested that a large collection of cosmic dust will be more representative of the earth-crossing meteoroid complex and represent a wider spectrum of solar system material than the conventional meteorites and therefore, can provide uniquely valuable information (Brownlee 1985; Brownlee et al. 1997).

We have made a large scale collection of cosmic spherules from the Indian Ocean using magnetic methods. In this paper we report on the morphological and petrographic

investigations carried out on 168 spherules collected by raking the surface sediments of the Indian Ocean along 5 tracks of ~ 4 km length each.

2 Sample Collection: MACDUC Experiment and Analysis

Spherules for this study were collected from Central Indian Ocean Basin, CIOB, sediments at water depths of >5000 m by a magnetic panel placed in a dredge which we call “Magnetic Cosmic Dust Collection” acronym “MACDUC” onboard AA *Sidorenko*, a research vessel chartered by the Government of India during its 22nd cruise (Oct–Nov 1999). The equipment comprised of an assembly of an aluminium panel on which five powerful (1,400 gal) bar magnets were fixed (Fig. 1a, b). This assembly was clamped inside a dredge primarily being used for bulk collection of manganese nodules in the CIOB (Fig. 1c, d).

Majority of the particles entering the earth become ferromagnetic because of magnetite formation due to friction during atmospheric entry and therefore can easily be attracted by simple hand held magnets (Brownlee 1985). This aspect has been utilized in almost all deep-sea collections so far. Therefore, the panel containing the magnets in the MACDUC experiment would encounter magnetic material in the sediment ploughed by the dredge during its traverse on the deep sea floor and it is expected that some of these magnetic material would be cosmic dust in the form of spherules and also some unmelted material similar to the ones collected in the stratosphere and in the polar regions.

Fourteen such operations were carried out in the CIOB during one cruise, each operation running for duration of ~ 10 h and the average distance traversed on the seafloor being ~ 4 km per operation at a very slow ship speed (Table 1). The dredge was dragged along the seafloor for 10–15 min and lifted up to 100 m above the seafloor and suspended in the deep sea for about 10 min to allow for the sediments collected in the dredge mouth to wash off. Subsequently, the dredge was lowered once again and dragged along the seafloor. The sequence of dragging and washing the sediment was done for 10–12 times during each operation. The material attracted by magnets was accumulated on the nylon cloth placed above them (Fig. 1e–g). The dimensions of the dredge used for the collection was 246 cm \times 70 cm. Assuming that the penetration of the dredge into deep seafloor sediments was up to its full width (70 cm), we consider here that the spherules could have a range of ages extending from 0 to 250,000 years based on the estimates from the sediment accumulation rates in the area (2.5–3.20 m/ 10^6 years: Prasad and Sudhakar 1999; Prasad et al. 2003). The retrieved material was carefully washed from the cloth in the lab, and was brought into slurry and was again subjected to magnetic separation. Out of the 14 operations carried out during the MACDUC experiment, >1245 spherules in the size range of 80–600 μm have been recovered from 852.7 mg of total magnetic fraction. The number of spherules isolated from each operation ranged from 47 to 189 (Table 1). There did not appear to be any relation between the amounts of time the dredge was dragged on the seafloor with number of spherules collected. However, in one operation (D8) where the dredge was dragged for a maximum distance of 14 km, 189 spherules were recovered which is the largest number among all the 14 tracks. A comparison of the present haul with other deep sea collections is given in Table 2.

For the present study, 598 spherules were handpicked from 5 different tracks with the aid of a binocular microscope having a magnification up to 80 \times and studied for their general surface features. Out of these, a total of 168 spherules were observed in a JEOL JSM 5800LV Scanning electron microscope to study their detailed external morphological,



textural features and, over 965 images have been obtained using both secondary (SEI) and backscatter electron image (BEI) modes. An observation in BEI mode generally enables distinguishing cosmic from terrestrial spherules. In addition, one hundred (~ 20 particles from each of the five tracks) black, angular particles were also analyzed for unmelted

◀ **Fig. 1** Magnetic cosmic dust collection (*MACDUC*) panel assembly and sampling. **a** The assembly comprising of an aluminium panel over which five bar magnets are placed, which are then covered by a non-magnetic metallic mesh, over which a nylon cloth is placed. **b** The assembly clamped with nylon cloth over the magnets. **c** *MACDUC* assembly being clamped to the side walls of the dredge used for bulk collection of manganese nodules from the ocean floor. **d** *MACDUC* panel on the wall of the dredge, ready for deployment. **e** Dredge along with the panel being lowered into deep sea floor. **f** *MACDUC* panel bathed with sediment and magnetic material after ploughing the deep sea floor. **g** Nylon cloth on panel after dredging shows deep sea sediments with magnetic fraction comprised of spherules and volcanic debris. **h** Binocular microphotograph of spherules recovered from one such operation. The largest spherule has a diameter of $\sim 600 \mu\text{m}$

cosmic material—all of them were terrestrial. Extraterrestrial nature of particles was primarily ascertained by using the physical and chemical measures laid down by Blanchard et al. (1980) and Brownlee (1981). The primary chemical compositions have been determined by analyzing spherule surface chemistry using Energy dispersive X-ray spectrometry (EDS). The cosmic spherules ($n = 115$) were further mounted in epoxy, sectioned and polished. Out of the 138 cosmic spherules observed, we could retrieve only 115 for polished section analysis—the rest were highly weathered and crumbled during retrieval. The internal features of spherules were observed in detail under SEM. Major element data was obtained using OXFORD-INCA Energy dispersive X-ray spectrometer at 20 keV acceleration and the same was quantified using automated ZAF program. Springwater meteoritic olivine standard (USNM 2566) provided by the Smithsonian Institution, Washington (Jarosewich et al. 1980) was used as a standard, especially for the S- and G-type spherules. The processing time used for analysis was 180–200 s with 8–12 kcps. Analytical accuracy was in the range 2–3.5% for major compounds and up to 10% for the minor oxide MnO which has a weight percent of 0.30.

3 Results

3.1 External Morphology and Internal Features

The collected magnetic fraction comprised of spherules and volcanic debris in the form of magnetite crystals, breadcrusts etc. Diameter of spherules varied from 55 to $\sim 600 \mu\text{m}$, with an average of $181.4 \mu\text{m}$ and standard deviation ± 15 . The average diameter is close to that observed by other investigators for extraterrestrial particulate matter (Love and Brownlee 1993; Taylor et al. 2000). External appearance of the spherules varied from very rough, earthy to smooth, shiny and spherules having metallic lustre (Fig. 1h). Most of the spherules were perfectly spherical in shape whereas some of them showed oval and bullet shapes.

For this study, 168 spherules were picked randomly from five tracks and analyzed for detailed morphological and textural features in the SEM. About 82% of the particles were cosmic in nature whereas the remaining were either volcanic spherules or manganese micronodules.

The spherules could be broadly characterized into three basic types namely I-type (33%), S-type (62%) and G-type (4.3%) on the basis of their textures and compositions. When compared with other deep sea collections, these percentages are similar (Table 3), however, the polar micrometeorite collections invariably have very low percentages of the I-type and G-type spherules ($\sim 1\%$) and a predominant portion of the collection (98%) are S-type spherules (Taylor et al. 2000). A strong magnetic bias is therefore dominant in the present

Table 1 Comparison of deep sea collections of cosmic spherules (modified after: Taylor and Lever 2001)

| Collection technique | No. examined | Size range (μm) | Presumed age | Reference |
|--------------------------|--------------|------------------------------|--------------|-----------------------------------|
| Cores | 100s | 60–500 | ? | Murray and Renard (1883, 1891) |
| Magnetic rake | >300 | 100–500 | ? | Bruun et al. (1955) |
| Core from top 3 m | 732 | 10–230 | <7 Ma | Laevastu and Mellis (1955) |
| Magnetic sieve | 4413 | 30–250 | <200 Ka | Pettersson and Fredriksson (1958) |
| 750 kg sieved, mag. sep. | 1200 | 149–351 | ? | Millard and Finkleman (1970) |
| Magnetic rake | 100s | <5000 | 0–100 Ka | Brownlee et al. (1979) |
| Mag. sep. box core | >700 | 100–1000 | 0–500 Ka | Blanchard et al. (1980) |
| 1 m clam shell sample | 935 | 149–750 | 0–700 Ka | Murrel et al. (1980) |
| 0–35 cm core, mag. sep. | 258 | 50–500 | 0–350 Ka | Kyte et al. (1983) |
| Magnetic rake | >138 | 55–650 | 0–250 Ka | MACDUC-present work |

Table 2 Comparison of percentages of spherule types between MACDUC spherules with that of Deep Sea Spherules (DSS) of Taylor and Brownlee (1991)

| Collection | Number of spherules studied | I-type (%) | S-type (%) | G-type (%) | Resumed age (K years) |
|--------------------------------|-----------------------------|------------|------------|------------|-----------------------|
| MACDUC (2007) | 138 | 33 | 62 | 5 | 0–250 |
| DSS (Taylor and Brownlee 1991) | 778 | 26 | 69 | 5 | <500 |

Table 3 Overview of spherules analyzed in this study

| Dredge no. | Total no. of spherules recovered | Spherules studied under SEM | No. of cosmic spherules | Number of spherules characterized | | |
|------------|----------------------------------|-----------------------------|-------------------------|-----------------------------------|--------|--------|
| | | | | I-type | S-type | G-type |
| AAS22/D1 | 135 | 20 | 14 | 3 | 11 | – |
| AAS22/D3 | 83 | 33 | 32 | 14 | 17 | 1 |
| AAS22/D7 | 101 | 30 | 11 | 3 | 7 | 1 |
| AAS22/D8 | 189 | 45 | 43 | 12 | 29 | 2 |
| AAS22/D10 | 90 | 40 | 38 | 14 | 22 | 2 |
| | 598 | 168 | 138 | 46 | 86 | 6 |

collection. This difference in abundance may also be due to a rapid weathering of chondritic particles in deep sea conditions (Kyte 1983). The S-type spherules in the present collection show high levels of etching, and barred olivine spherules show maximum etching effects among all the spherules examined. Taylor et al. (2000) calculated the global accretion rates for stony ($1,000 \pm 300$ tonnes year⁻¹) and I-type spherules (40 ± 15 tonnes year⁻¹) from SPWW cosmic spherules and compared these with other DSS spherules. Accretion rates (in tonnes year⁻¹) of S-type spherules collected from deep sea are lower [Murrell et al. (1980), 90 ± 45 ; Kyte (1983), 370 ± 190 ; DSS Box Core, 35 ± 25] than that of SPWW spherules. They also suggested that the terrestrial weathering is not the only reason for high abundance of I-types in deep sea spherules, a strong magnetic bias in the collection could also

Table 4 Composition of metal beads and glass encased void portions in exposed cross-sections of I-type spherules

| Sample No. | Description of feature | Fe | Ni | Co | Si | Mg | Al | Ca | Cr |
|----------------|------------------------------------|-------|-------|------|-------|------|------|------|------|
| AAS22/D1, P7 | Fe–Ni bead | 32.60 | 43.02 | 2.53 | ND* | ND | ND | ND | ND |
| AAS22/D3, P1 | Fe–Ni bead | 67.98 | 9.09 | ND | 0.24 | 0.32 | ND | ND | ND |
| AAS22/D3, P8 | Fe–Ni bead, bright portion | 7.76 | 70.73 | ND | ND | ND | ND | ND | ND |
| AAS22/D3, P8 | Fe–Ni bead, dark portion | 7.58 | 69.26 | 0.52 | 0.42 | 0.33 | ND | ND | ND |
| AAS22/D3, P8 | Glassy portion adjoining void area | 53.24 | 2.12 | ND | 3.93 | ND | 9.78 | 1.37 | ND |
| AAS22/D3, P13 | Glassy portion adjoining void area | 3.02 | ND | ND | 38.61 | ND | 5.61 | 1.06 | ND |
| AAS22/D8, P18 | Glassy portion adjoining void area | 69.27 | 7.72 | ND | 0.33 | ND | ND | ND | 0.24 |
| AAS22/D10, P10 | Fe–Ni bead | 74.98 | 2.58 | ND | ND | ND | ND | ND | 0.18 |
| AAS22/D10, P7 | Glassy portion adjoining void area | 46.09 | 3.34 | ND | 11.81 | 2.54 | ND | 1.43 | 3.40 |
| AAS22/D10, P11 | Fe–Ni bead | 62.26 | 15.64 | ND | ND | ND | ND | ND | ND |

* Not detected

concentrate these types of spherules. An overview of spherules studied during this work is given in Table 4.

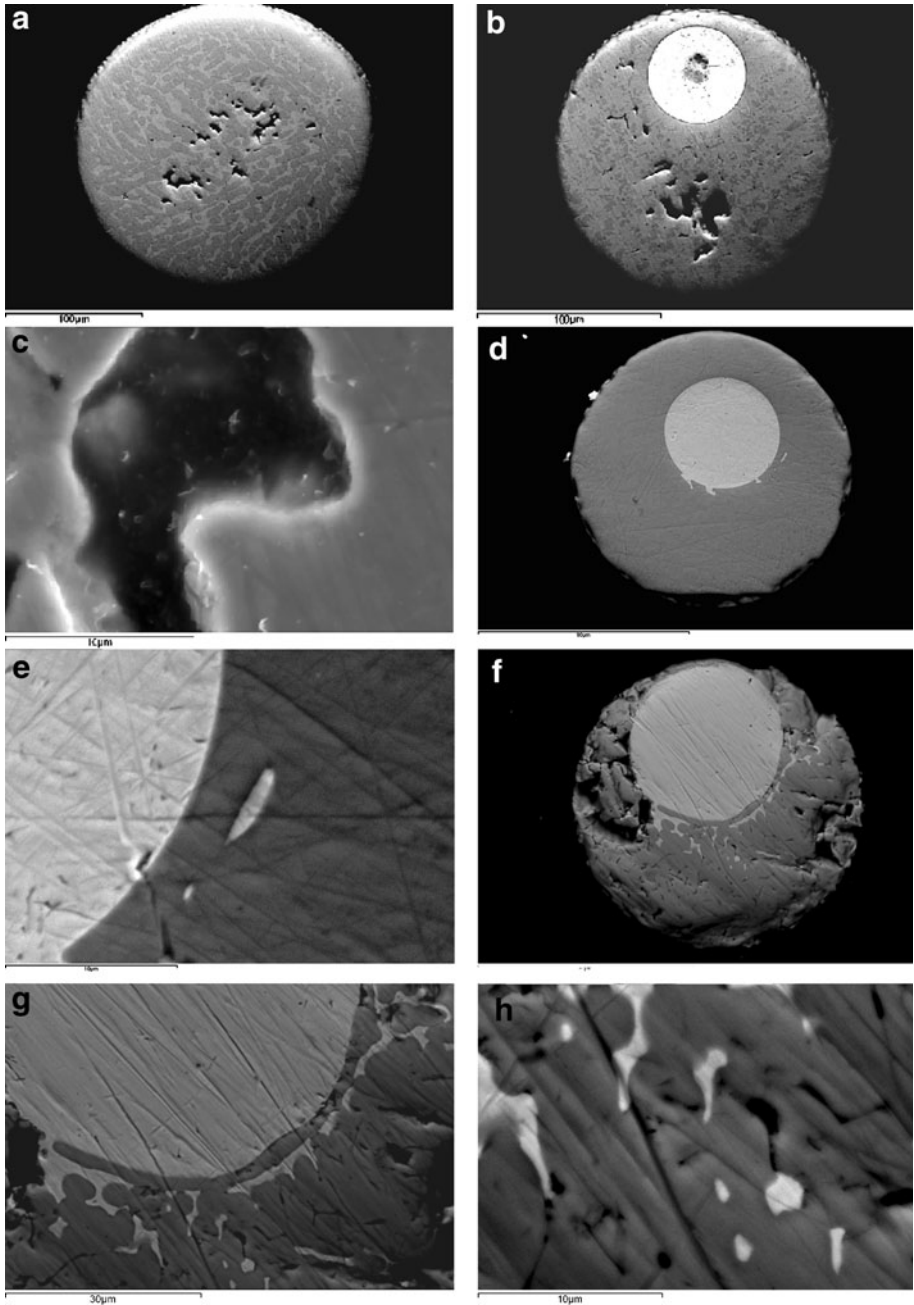
3.2 I-Type Spherules

These constitute 33% of all analyzed particles; they are of relatively smaller diameters, mostly spherical, smooth, shiny black and composed of brickwork of magnetite crystals on their surfaces. They are easily identifiable on the basis of their high nickel contents along with Fe and some cobalt.

In the present collection we characterized 46 I-type spherules out of which 19 had a Fe–Ni bead. The other 25 were without a Fe–Ni bead which is not surprising because during atmospheric entry metal is released from the meteoroids. The bulk composition of all the spherules shows Fe and varying percentages of Ni (0.5 to ~6%) which are within the known range for I-type spherules (Herzog et al. 1999). The wustite portions of all the spherules show approximately 1.5 times more nickel contents than the magnetite portions.

Spherules without metallic core: Out of the 25 such spherules observed, four contained platinum group nuggets (Parashar and Prasad, 2008; Rudraswami et al. 2010). In the spherules without a metal bead the Ni content is very low (<0.5%) and these have a dominant magnetite phase (dark portions in Fig. 2a) and invariably contain uneven shaped voids closer to the center of the spherule (voids are seen in the spherules with beads as well). The voids have glassy outlines which contain lithophiles such as Mg, Si, Ca and Al (Table 4; Fig. 2c). These void spaces were suggested to have been generated either due to shrinkage or escape of volatile elements during atmospheric entry (Feng et al. 2005).

Spherules with metallic core: Some of these cores were at the edge of the spherules and could be seen in the exposed spherules (Fig. 2a). In a majority of the cases, Fe–Ni core comprised dominantly of Fe and Ni, however two such cores showed the presence of cobalt (Table 4; Fig. 2b, d). In one of the cores (Fig. 2d), high percentage of cobalt (2.5%) is seen which is distributed uniformly throughout the core, and also similar percentages of cobalt are found in the metal blebs close to the metallic core. The nickel content in this core is 43% and as such the Ni/Co is closer to the chondritic ratio of 20 (Tagle and Berlin 2008). However in D3, P8 (Fig. 2b) the bright portion of the core has a uniform composition of Fe (7.76%) and Ni (70.73%), whereas there is a dark patch observed at the center of the core



(in the BEI image) which shows presence of cobalt (0.52%) in addition to small percentages of lithophiles such as Mg (0.33%), and Si (0.42%) and Co (0.52%). Here, the Ni/Co ratio is nowhere near chondritic. The presence of lithophiles here probably also point towards a parent body which may not have been an iron meteorite. In support of this

◀ **Fig. 2** I-type spherules: **a** Polished section of an I-type spherule without a Fe–Ni core, the dark portions are magnetite and the lighter portions are wustite. The uneven voids in the center sometimes contain a glassy cover which shows lithophiles. **b** I-type spherule with wustite portion dominant and a large Fe–Ni core. The darker portions near the center of the core contain Co, Si and Mg in addition to Fe and Ni. **c** Glassy cover on the void portion of spherule shown in ‘b’. Such glassy portions show appreciable amounts of Si, Al, and Ca (Table 4). **d** Wustite dominant I-type sphere with a large Fe–Ni core. This core is enriched in Cobalt (Table 4). **e** Metal bleb near the metallic core shown in “c”. The bleb has similar composition as that of the metallic core. **f–h** Spherule with the largest metallic core observed in this study. The metal is being accumulated in the form of metallic blebs surrounding the core

argument, the void portion of this spherule also contains glassy sheath which has Si, Ca and Al (Table 4; Fig. 2c).

The Ni contents in the cores showed large variations from ~3 to ~80% and the size of the core has no bearing on the total Nickel content, for example, in D10, P11 (Fig. 3f–h) although has the largest core observed in this study, the total nickel content in bead is only 15.6%, which is much lower than that of D1 P7 (Fig. 2d)—which has a smaller bead but with much higher nickel content :40.69%.

In the metallic cores with low Ni contents, the boundary between the rest of the spherule and the core is often not sharp (e.g. Fig. 3b), this is in contrast with cores having higher nickel contents where a sharp boundary exists between the surrounding spherule and the bead (e.g. Fig. 2b). In two such spherules (Fig. 2d, e), metal blebs are seen closer to the core (Fig. 2d) and surrounding the core (Fig. 3f–h). which appear to be in the process of merging with the Fe–Ni bead. All these metallic blebs and the Fe–Ni core have similar compositions (Table 4).

3.3 G-Type Spherules

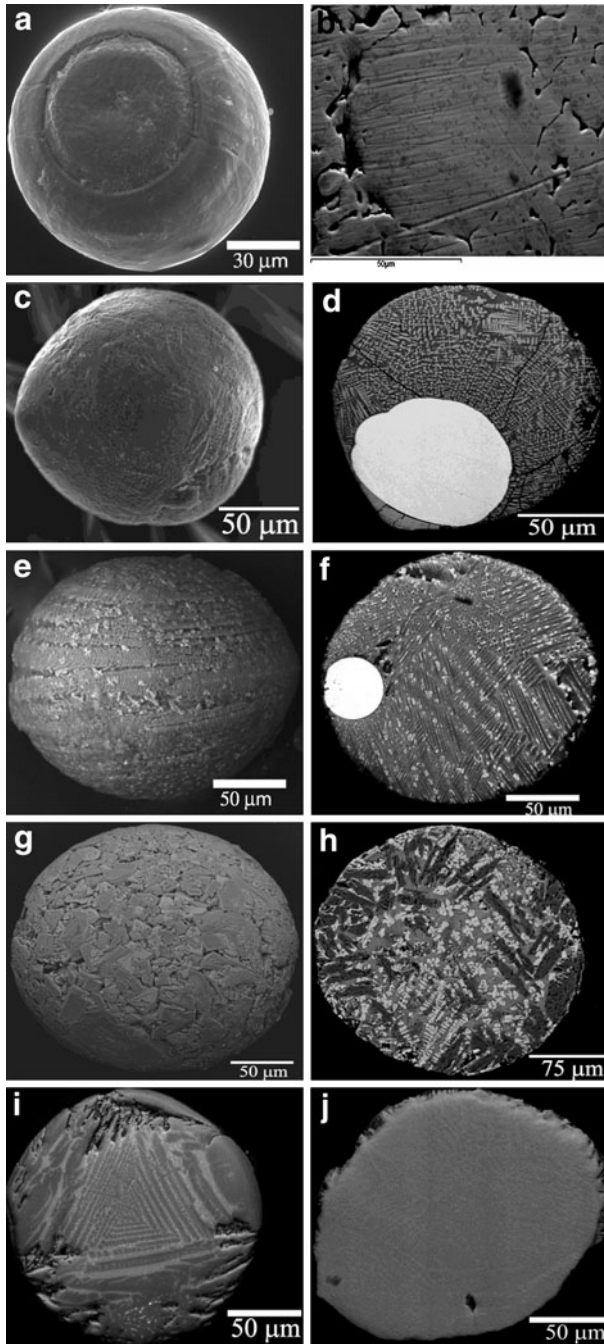
Approximately 5% of all deep sea spherules are of the G-type whereas, the percentages are lower in the polar collections. The G-types in the present collection show smooth surface textures with metallic lustre (Fig. 3c). Their internal features reveal continuous dendritic magnetite crystals in a silicate glass matrix; occasionally the spherules also show an eccentric Fe–Ni metal core (Fig. 3d). G-type spherules show very high concentration of FeO (68.97 ± 6.22 wt%) with mesostasis showing MgO (7–11 wt%), Al₂O₃ (0.5–1.2 wt%), SiO₂ (11–22 wt%), CaO (6–9 wt%) and NiO (~4 wt%) (Table 5).

3.4 S-Type or Stony Spherules

S-type spherules are the most dominant group (62%) in the collection and are typically composed of olivine and magnetite crystals with interstitial glass. These S-type spherules are further divided into subgroups, which generally reflect the various levels of heating experienced during atmospheric entry (Taylor et al. 2000; Genge et al. 2008). Taylor et al. (2000) classified S-type spherules in the order of the heating and melting experienced, where scoriaceous spherules are the least heated followed by relic-grain bearing, porphyritic, barred, cryptocrystalline, glass and CAT spherules which have experienced the maximum heating during entry and therefore, have a high percentage of the refractory elements calcium, aluminium and titanium (Table 6).

We have not come across either a scoriaceous spherule or a CAT spherule in this collection so far. The other S-type spherules in this collection are described below:

Relic grain bearing (RGB) spherule: We found only one RGB (300 μm diameter) so far in this collection, which contained a two chromite grains of apparently similar sizes, one of



which is $\sim 43 \mu\text{m}$ in size (as ascertained in the polished section) within an Mg–silicate matrix (Fig. 4a). The spherule is oval-shaped having an etched surface where large dendritic magnetites, silicate phases and two relict chromite grains could be distinguished in

◀ **Fig. 3** External morphology and internal features of cosmic spherules. **a** Smooth surfaced I-type spherule and, **b** its *polished section* showing FeNi core; **c** G-type spherule with a smooth exterior and, **d** its *polished section* showing an eccentric FeNi metal core, dendritic magnetites and mesostasis comprising dominantly of lithophiles; **e** Barred olivine spherule with olivine lathes and mesostasis with magnetite seen, the interstitial glassy area is largely etched out and, **f** its *polished section* with a Fe–Ni metal bead at the edge; **g** Porphyritic olivine spherule with zoned olivines and the mesostasis is etched out due to seawater action and, **h** its *polished section* with zoned olivines, mesostasis of glass and magnetites seen; **i** *Polished section* of a cryptocrystalline spherule. Spherule shows a “cobweb” type of structure with *light and dark concentric banding*, where the dark portions are more Mg-rich and show forsteritic compositions whereas the light coloured bands show more fayalitic composition. Bright spots at the bottom edge of the spherule are magnetites; **j** *Polished section* of a glassy spherule, no visible crystals of olivine or magnetite

the BEI mode of the SEM (Fig. 4a). On the surface of the spherule, one of the relict chromites appears larger in size, however, a larger portion of this grain could be exposed. Both the chromites show similar composition. During polishing the larger chromite grain has been lost and the ‘smaller’ one is seen to measure $\sim 43 \mu\text{m}$ (Fig. 4b, c). This grain is idiomorphic, and is enriched in Cr_2O_3 with some lithophiles and also shows prominent rim (Fig. 4b, c) where chromite is gradually replaced by magnetite. The rim apparently crystallized subsequent to melting in the atmosphere. Chromite in view of its highly refractive nature could have survived atmospheric heating and was retained as relic grain in the spherule.

Porphyritic or equant olivine spherules constitute 13% of stony spherules and have subhedral to euhedral zoned olivine crystals with magnetite in interstitial glass (Fig. 4g, h). The porphyritic olivine spherules contain zoned olivine crystals (Fo43–88) with Mg-rich cores (Fo62–88) and Fe concentrated in the rims (Fa14–55) (Table 7). The sizes of zoned olivines ranges from 3 to 70 μm and the larger crystals show greater differences in MgO and FeO contents between the rims and the cores compositions due to zoning (Fig. 5).

Barred olivine spherules are the most common (78%) among the stony types which show elongated, bar-shaped olivine and dendritic magnetite crystals with interstitial glass (Fig. 3e). These spherules, on some occasions, contain spherical vesicles—such void spaces have been suggested to have been occupied by volatile elements which escaped during atmospheric entry (Blanchard et al. 1980). Some spherules contain eccentric FeNi metal beads (Fig. 3f). Particles with Fe–Ni bead are not very uncommon and have been reported earlier by other authors, for example, Taylor et al. (2000) found 11% of the chondritic spherules from their South Pole collection contain one or more Fe–Ni metal beads. We found three such particles which show olivine composition and an eccentric FeNi metal bead (Fig. 3f) where metal segregation is suggested to have taken place during the atmospheric entry due carbon burning under low oxygen fugacity conditions leading to reducing conditions (Genge and Grady 1998).

We also found spherules which show both barred olivine as well as porphyritic olivine textures in the polished section and can be regarded as transitional between the PO and BO types of spherules. In addition, two spherules show flattened, circular droplets having high Fe–Ni contents (Ni = 58%; Fe = 9%) welded to the surface of the spherule. Another such spherule shows a microcrater-like depression which has enhanced Fe ($\sim 75\%$) and Ni ($\sim 0.76\%$) where the host spherule has 49% and 0.25% percent respectively of the same elements. These features are also Fe–Ni metal that gets segregated during atmospheric entry leading to siderophile depletion observed in stony spherules.

Cryptocrystalline spherule was found with zoned ‘Cobweb’ structure which represents domains of differently oriented olivine dendrites (Fig. 3i). The particle shows alternate bands of light and dark colours. Dark bands show forsteritic (Fo61–87) composition

Table 5 Major element composition (wt%) of stony and G-type spherules analyzed by EDS

| Type | MgO | Al ₂ O ₃ | SiO ₂ | CaO | Cr ₂ O ₃ ^a | MnO ^b | FeO | NiO ^c |
|-----------------------------------|---------------|--------------------------------|------------------|--------------|---|------------------|---------------|------------------|
| RGB (<i>n</i> = 1) | 26.13 | BD | 38.02 | 0.47 | 0.27 | 0.61 | 34.50 | BD |
| Porphyritic (<i>n</i> = 6) | 27.72 (±4.60) | 1.95 (±0.64) | 36.57 (±1.92) | 1.55 (±0.69) | 0.57 (±0.08) | 0.59 | 31.24 (±4.13) | 1.18 (±0.43) |
| Barred olivine (<i>n</i> = 34) | 25.28 (±3.00) | 2.53 (±1.39) | 38.27 (±4.22) | 1.71 (±0.79) | 0.61 (±0.14) | 0.48 | 31.45 (±6.04) | 1.27 (±0.75) |
| Cryptocrystalline (<i>n</i> = 2) | 26.05 ± 4.73 | 2.27 ± 0.29 | 40.88 ± 8.81 | 2.80 ± 1.14 | BD | 0.58 | 27.90 ± 15.13 | BD |
| Glassy (<i>n</i> = 3) | 25.63 (±3.09) | 3.09 (±0.86) | 42.09 (±1.64) | 2.13 (±0.57) | BD | 0.36 | 25.96 (±2.09) | BD |
| G-type (<i>n</i> = 3) | 10.44 (±3.07) | 0.74 (±0.40) | 17.48 (±5.49) | 0.70 (±0.17) | 0.56 | BD | 68.97 (±6.22) | 4.75 |

BD below detection limit

^a Cr₂O₃ detected in 19 spherules

^b MnO detected in 12 spherules

^c NiO detected in 28 spherules

Table 6 Chemical composition of relict grain bearing spherule, and chromite relict grain

| | Mg/ Si | Ca/Si | Fe/Si | | | | | | | |
|--|-----------|--------------------------------|------------------|-----|-------------------------------|------------------|--------------------------------|------|-------|--|
| Bulk spherule | 0.95 | 0.012 | 0.708 | | | | | | | |
| H Chondrite ^a | 0.96 | 0.052 | 0.818 | | | | | | | |
| L Chondrite | 0.93 | 0.005 | 0.584 | | | | | | | |
| | MgO | Al ₂ O ₃ | SiO ₂ | CaO | V ₂ O ₅ | TiO ₂ | Cr ₂ O ₃ | MnO | FeO | |
| Chromite grain: core | 7.3 | 12.69 | – | – | 0.71 | 0.58 | 53.72 | 0.65 | 24.86 | |
| Chromite grain: rim | 8.91 | 0.92 | – | – | ND | ND | 6.11 | 0.44 | 80.91 | |
| Chromite in L3 chondrite ^b Krymka B | 8.4 | 12.6 | – | – | 0.82 | 0.6 | 53.2 | 0.59 | 23.4 | |
| Chromite in H chondrite ^c | 3.4 | 6.64 | – | – | 0.65 | 1.96 | 57.7 | 0.88 | 28.9 | |
| Chromite in L chondrite | 2.52 | 5.9 | – | – | 0.7 | 2.67 | 56.1 | 0.63 | 30.9 | |
| Chromite in LL chondrite | 1.85 | 5.52 | – | – | 0.67 | 3.4 | 55.8 | 0.51 | 31.6 | |
| Extraterrestrial chromite grains (594) ^d | 2.57 | 5.53 | – | – | 0.73 | 2.73 | 57.6 | 1.01 | 26.94 | |

^a H chondrite and L chondrite averages from Wasson and Kallemeyn (1988)

^b Chromite in L3 chondrite Krymka B from Bunch et al. (1967)

^c Chromite in H, L, and LL chondrites, data from Wlotzka (2004)

^d Extraterrestrial chromite grains (594) from Schmitz et al. (2001)

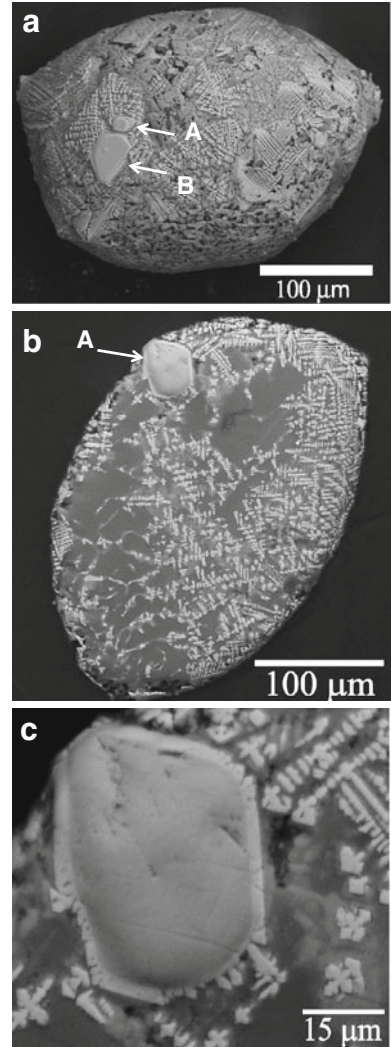
whereas; light coloured bands show fayalitic (Fa48-57) composition. The spherule also shows formation of small magnetite crystals in clusters.

Glassy spherules constitute 7% of spherules, they have smooth surface textures and show no crystals of either olivine or magnetite but show stony spherule compositions (Fig. 3j). Glassy spherules show comparatively high amount of SiO₂ (>41% wt%). Magnetite crystals present in between the olivine are submicron to few microns in size and are mainly composed of Fe with little amounts of Al, Ti, and Cr. The glass composition is predominated by the Fe whereas the Mg, Si, Ca, Al are the other minor constituents.

3.5 Major Element Composition Trends

Stony and G-type spherules were analyzed for their major element compositions. In cases where the spherules show etching effects, only unetched central portions were analysed. Major elements detected by EDS under standard conditions show strong peaks for Mg, Al, Si, Ca, and Fe. While Mn, Cr and Ni were detected in few particles, Ti was below the detection limit of the system (Table 5). These particles when plotted on Mg–Si–Fe (atom) ternary diagram (Fig. 6), display olivine normative compositions dispersed around forsterite-fayalite line as seen in the deep sea spherules of Brownlee et al. (1997). G-type spherules tend towards the Fe-end because of their high iron content. These spherules show higher concentrations for Fe in comparison to the spherules collected from polar ices. The Si-normalized mean compositions for the elements Mg, Al, Ca, and Fe detected in the spherules, as shown by histograms (Fig. 6), are very close to the mean CI values (Table 8)

Fig. 4 Relict grain bearing spherule: **a** BEI image of a silicate spherule with two relict chromite crystals (*arrows* point towards the two grains); **b** Polished section of the spherule showing idiomorphic chromite grain with a zoned rim. This grain is the smaller grain observed in **a** where only a part is exposed. **c** Relict chromite grain under higher magnification. Zoned rim of the crystal contains higher Fe contents indicating equilibration with the surrounding magnetite-rich area of the spherule



but the elements like Cr, Mn and Ni though not detected in all particles show high degree of depletion relative to chondritic values (Fig. 7).

4 Discussion

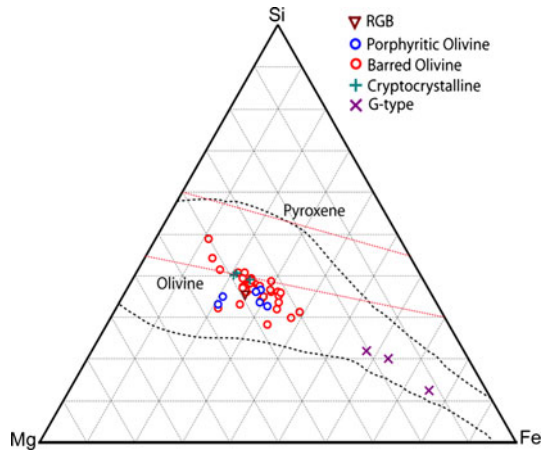
Out of the 138 spherules studied here, 33% are of the I-type which is higher when compared with other DSS collections (Table 2), 62% of the spherules are S-type and 5% are of the G-type.

I-type spherules: I-type spherules were amongst the first to be recognized as cosmic (Marvin and Einaudi 1967; Millard and Finkleman 1970) especially in view of their high nickel contents and presence of wustite which is a metastable iron mineral ($\text{Fe}_{(1-x)}\text{O}$) which forms under low oxygen partial pressure during atmospheric entry (Brownlee et al.

Table 7 Compositions of olivine in porphyritic spherules

| | MgO | Al ₂ O ₃ | SiO ₂ | CaO | FeO | NiO | Fo/Fa |
|--------|-------|--------------------------------|------------------|------|-------|------|-------------|
| D3P5 | | | | | | | |
| Core | 40.50 | ND | 40.38 | 0.28 | 17.56 | 1.28 | 80.44/19.56 |
| Rim | 31.13 | ND | 37.30 | 0.53 | 29.41 | 1.63 | 65.36/34.64 |
| D8P19 | | | | | | | |
| Core | 42.44 | ND | 41.69 | ND | 12.4 | 2.47 | 85.92/14.08 |
| Rim | 16.97 | 1.82 | 39.85 | 2.27 | 38.11 | 0.33 | 43.83/55.21 |
| D8P28 | | | | | | | |
| Core | 41.25 | ND | 40.66 | ND | 14.36 | 3.72 | 83.66/16.34 |
| Rim | 25.62 | 1.53 | 42.81 | 1.34 | 27.69 | 1.01 | 62.26/37.74 |
| D10P15 | | | | | | | |
| Core | 42.81 | ND | 41.35 | ND | 14.17 | 1.14 | 84.34/15.66 |
| Rim | 26.50 | 1.43 | 40.24 | 1.13 | 29.10 | 1.15 | 61.88/38.12 |

Fig. 5 Mg–Fe–Si (atom) ternary plot for MACDUC cosmic spherules; dashed line indicates the known range in composition of cosmic dust plotted from data after Brownlee et al. (1997), Taylor et al. (2000), and Badjukov and Raitala (2003)



1975). Many investigators assigned a chondritic parent body for I-type spherules (e.g. Blanchard et al. 1980). The metal that comprises an I-type spherule is proposed to have been originated due to frictional heating of carbonaceous chondritic material in the presence of carbon under low oxygen fugacity which led to reducing conditions (Brownlee et al. 1983, 1997). The metal thus produced separated from the silicate portions due to inertial forces (Blanchard et al. 1980).

Carbonaceous chondrites contain chondrules, matrix and metal in different proportions. Herzog et al. (1999) suggested that most type I spherules are atmospherically processed metal grains from carbonaceous/unequilibrated chondritic bodies. This is supported by the presence of cosmogenic radionuclides in I-type spherules which indicates that they could have been primary bodies in space and have undergone a minimum of mass loss which is estimated at ~30% (Nishiizumi et al. 1995) this mass loss is similar to that of a barred olivine spherule (Hashimoto 1983).

The presence of large metallic cores with high percentages of Ni and Co in the present study, along with the presence of lithophile elements within the spherules are all supportive

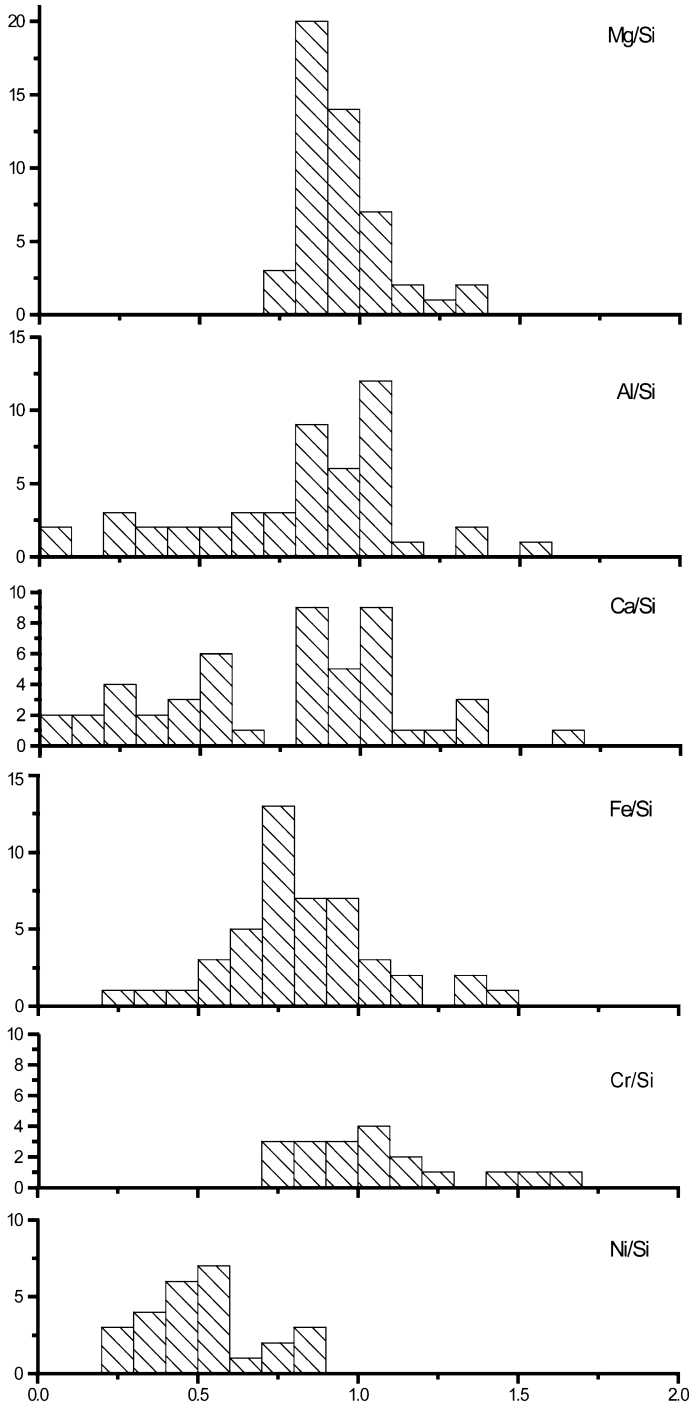


Fig. 6 Element to Si ratio normalized to CI values. *Dashed line* indicates the mean CM chondrite composition (Wasson and Kallemeyn 1988)

Table 8 Bulk elemental ratios of MACDUC cosmic spherules in comparison with DSS and chondrites

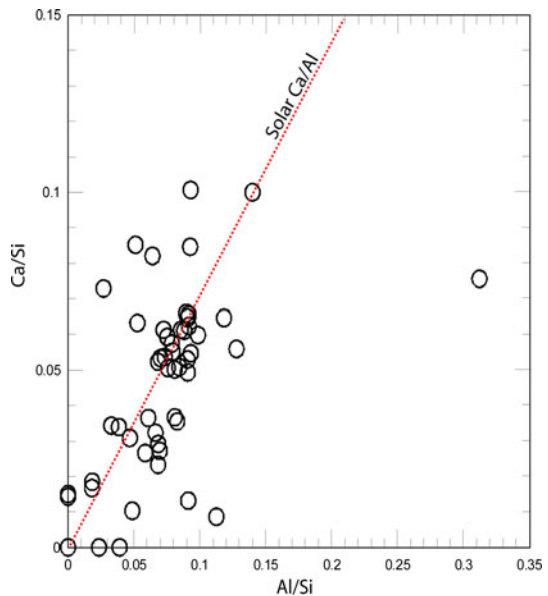
| | Mg/Si | Al/Si | Ca/Si | Fe/Si | Ni/Si |
|--------|-------|-------|-------|-------|-------|
| MACDUC | 1.01 | 0.074 | 0.047 | 0.934 | 0.022 |
| DSS | 1.06 | 0.083 | 0.059 | 1.024 | 0.019 |
| CI | 1.07 | 0.085 | 0.061 | 0.90 | 0.049 |
| CM | 1.05 | 0.095 | 0.069 | 0.819 | 0.045 |
| H | 0.96 | 0.07 | 0.052 | 0.818 | 0.045 |
| L | 0.93 | 0.069 | 0.05 | 0.584 | 0.031 |

DSS Average from Brownlee et al. (1997)

CI Chondrite average from Anders and Gravenes (1989)

CM, H, and L chondrite averages from Wasson and Kallemeyn (1988)

Fig. 7 Calcium vs. Aluminium (atom) normalized to Si for S- and G-type spherules in this study. Solar Ca/Al ratio is also shown for comparison



of the origin proposed by Herzog et al. (1999) that these spherules could have been processed metal grains from chondritic parent bodies.

S-type and G-type spherules: The overall bulk compositions of the S-type spherules conforms to the other large cosmic spherule collections from diverse environments (Koeberl and Hagen 1989; Brownlee et al. 1997; Taylor et al. 2000; Badjukov et al. 2003). The gradual fall in Si-normalized Fe values from RGB to glass (RGB-1.50; PO-1.42; BO-1.35; glass-1.03) with progressive heating supports the suggestion that the increasing loss of Fe from chondritic particles leads to compositional and textural changes in completely melted spherules (Hashimoto et al. 1979; Hashimoto 1983).

There are three principal phases in these spherules namely, olivine, magnetite and glass. The barred olivine generally shows skeletal or lath shaped crystals with composition ranging from Fa_{20} to Fa_{50} . In many cases, these barred olivines are not fully equilibrated and show a wide range of MgO–FeO compositions.

G-type spherules were considered to be intermediate between I and S-types earlier (Blanchard et al. 1980). These particles however, comprise of high Fe contents with continuous dendrites of magnetites throughout the spherules in a silicate matrix and they have a very low-Mn/Si ratios because of which, Brownlee et al. (1997) suggested that the silicate component does not have a chondritic composition. Based on their minor element compositions, Bates (1986) suggested that these particles are similar to the metal silicate fractions of enstatite chondrites or achondrites. Brownlee et al. (1997) believe that it is not easy to match the G-type spherules with any particular chondrite; they could even be samples from a distinct enstatite-metal-rich asteroid type.

Siderophile depletion of elements like Ni, Cr, and Fe etc. relative to carbonaceous chondritic composition is a common feature among all S-type spherules. The initial process of siderophile segregation takes place under low oxygen fugacity, during entry due to rapid heating and reduction of the parent carbonaceous chondrite by pyrolysis (Brownlee et al. 1983). This has been confirmed during heating and vaporization experiments of carbonaceous materials (Hashimoto et al. 1979). The Si-normalized Ca and Al display a tendency towards solar Ca/Al compositions (Fig. 6) as observed by other investigators (Blanchard et al. 1980; Brownlee et al. 1997; Taylor et al. 2000). The drift in the Ca values relative to chondritic values may be attributed to the heterogeneity in the parent body itself (Brownlee et al. 1997), however the etching effects in deep sea spherules may again play an important role as the glass which contains most of Ca is lost because of the long residence time under sea water.

Relict chromite grains in the RGB spherule: could be important because an ordinary chondritic parent body could be assigned unambiguously. The most common relict minerals observed in micrometeorites are olivine, pyroxene, metals, sulfides, spinels, magnetite, and also chromite. Among these, sulphides, Fe–Ni metal grains and chromite grains are less common (Beckerling and Bischoff 1995). Beckerling and Bischoff (1995) carried out a focused study of relict grains from 227 antarctic micrometeorites (AMM) and found ~25% of the AMMs contain relict mineral grains. Taylor et al. (2000) found ~12% of their AMMs to be RGB spherules. Among the deep sea collections, Blanchard et al. (1980) could observe <10% of the spherules to contain relict mineral grains. Relict grains are the high temperature mineral granulates which escape melting during atmospheric heating and therefore, they give most direct clues to the nature and types of parent bodies (Brownlee 1985; Beckerling et al. 1993; Beckerling and Bischoff 1995) but also provide important clues to the atmospheric entry processes—especially from the grains that are not completely equilibrated with the host spherules.

Further, 87% of meteorites are ordinary chondrites and only 2.9% comprise of carbonaceous chondrites (Krot et al. 2005), whereas micrometeorites show a reverse trend where, 70% show affinity to carbonaceous chondrite parent bodies which are either CI or CM (Brownlee et al. 1997; Kurat et al. 1994) or objects with an affinity for CR chondrites (Engrand and Maurette 1998). A small fraction shows affinity to unequilibrated ordinary chondrites (Genge and Grady 2002; Robin et al. 1990; Brownlee et al. 1997). Genge and Grady (2002) suggest ~30% of micrometeorites to be derived from ordinary chondrite parent bodies. Very small percentages, as reported recently by Taylor et al. (2007) appear to have been derived from achondritic parent bodies.

Chromite although not very common in carbonaceous chondrites as well as iron meteorites, it is a common trace mineral in most ordinary chondrites (0.05–0.5%) (Schmitz et al. 2001; Rubin 1997). Further, its composition even within ordinary chondrites varies within narrow ranges for H, L, or LL type chondrites (Wlotzka 2005; Bunch et al. 1967) therefore becomes a good tracer to identify parent chondrite. Wlotzka (2005) in ordinary

chondrites occurs in two main forms: (1) As interstitial grains in the matrix, xenomorphically occurring within a silicate matrix and shows idiomorphic shapes only when in contact with troilite or metal. This form of chromite comprises large crystals (sizes up to hundred of micrometers). (2) As small grains disseminated within chondrules with dimensions of a few micrometers.

The sizes of the chromite grains ($\sim 43 \mu\text{m}$), and both occurring in a silicate mesostasis, in addition to the idiomorphic shapes of the grains encased in metal (magnetite) in the present RGB spherule suggest that they were part of the mesostasis of a chondritic body. However, the chemical composition of the chromite grains in the present study does not have any resemblance to the chromite grains studied extensively from ordinary chondrites (Schmitz and Haggstrom 2006) because the grain here has much higher MgO and Al₂O₃ contents, lower Cr₂O₃, FeO and TiO₂ contents (Table 6). This grain (the one analysed in the polished section) has a very close resemblance to the chromites found in the L3 chondrite Krymka B analysed by Bunch et al. (1967). The chromites in this chondrite were considered anomalous and “drastically different” as compared with those of other ordinary chondrites.

The bulk composition of the chromite bearing spherule however has atomic ratios which are close to that of ordinary chondrites (Table 6). The parent body of this particular spherule could be an ordinary chondrite—in all probability an L3 chondrite.

5 Conclusion

Raking deep sea floor sediments, a large scale collection of cosmic spherules was made. Out of 168 spherules observed for this study 138 were found to be cosmic. The collection is dominated by silicate or S-type spherules (62%), followed by the I-type which comprise of 33% and a small percentage of the G-types spherules are identified. The higher ratio of I-type spherules could be attributed to their greater resistance to weathering under sea water or due to the magnetic bias in the collection method. The presence of lithophile elements and the metal contents of the I-type spherules supports the argument that these could be metal grains from chondritic parent bodies. While a sequence of heating experienced by the S-type spherules is discernible by the various categories of S-type spherules observed here, there are also some which show stages intermediary between these main categories such as semi-porphyritic/barred spherule. Cosmic spherules analyzed in this study have elemental abundances similar to those investigated earlier by various workers and correspond to extraterrestrial samples, though, have been altered chemically/physically by atmospheric entry processes and also by exposure to terrestrial environments. The elemental ratios correspond to their derivation from CI and CM carbonaceous chondritic bodies mostly. One relict-grain bearing spherule has a chromite grain which has a ‘drastically different’ composition and the spherule strongly suggests an H or L chondrite as a parent body.

Acknowledgments The authors thank the Director, NIO Goa for the encouragement and support for this work. We express our gratitude to Gavin Walker and Joselan Pereira for their invaluable help during the collection of samples onboard AA *Sidorenko*. The authors are also grateful to Vijay Khedekar for his technical support during the SEM work. We are indebted to L. Folco and an anonymous reviewer for their incisive reviews and valuable suggestions. We also thank Joseph A. Nelen, Smithsonian Institution, Washington for providing meteorite mineral standards. This research has made use of NASA’s Astrophysics Data System. This project is funded by ISRO-PRL, Ahmedabad under the PLANEX program. This is NIO’s contribution number 4835.

References

- A. Anders, E. Gravesse, *Geochim. Cosmochim. Acta* **53**, 197 (1989)
- D.D. Badjukov, J. Raitala, *Meteorit. Planet. Sci.* **38**, 329 (2003)
- B.A. Bates, *The Elemental Composition of Stony Extraterrestrial Particles from the Ocean Floor*. Ph.D. Thesis, University of Washington, 1986, pp. 196
- M.B. Blanchard, D.E. Brownlee, T.E. Bunch, P.W. Hodge, F.T. Kyte, *Earth Planet. Sci. Lett.* **46**, 178 (1980)
- W. Beckerling, W. Klock, A. Bischoff, *Meteoritics* **28**, 320 (1993)
- W. Beckerling, A. Bischoff, *Planet. Space Sci.* **43**, 435 (1995)
- D.E. Brownlee, M.B. Blanchard, G.C. Cunningham, R.H. Beauchamp, R. Fruland, *J. Geophys. Res.* **80**, 4917 (1975)
- D.E. Brownlee, L.P. Pilachowski, P. Hodge, *Lunar Planet. Sci. Conf.* **10**, 157 (1979)
- D.E. Brownlee, in *The Sea*, 7th edn., ed. by E. Emiliani (Wiley, New York, 1981), p. 733
- D.E. Brownlee, B. Bates, R.H. Beauchamp, in *Chondrules and Their Origins*, ed. by E.A. King (Lunar and Planetary Institute, Houston, 1983), p. 10
- D.E. Brownlee, *Annu. Rev. Earth Planet. Sci.* **13**, 147 (1985)
- D.E. Brownlee, B. Bates, L. Schramm, *Meteorit. Planet. Sci.* **32**, 157 (1997)
- A.F. Bruun, E. Langer, H. Pauly, *Deep Sea Res.* **2**, 230 (1955)
- T.E. Bunch, K. Keil, K.G. Snetsinger, *Geochim. Cosmochim. Acta* **31**, 1569 (1967)
- J. Czajkowski, P. Englert, A. Bosellini, J.G. Off, *Meteoritics* **18**, 286 (1983)
- C. Engrand, M. Maurette, *Meteorit. Planet. Sci.* **33**, 565 (1998)
- H. Feng, K.W. Jones, T. Tomov, B. Steward, G.F. Herzog, C. Schnabel, D.E. Brownlee, *Meteorit. Planet. Sci.* **40** (2005)
- G.J. Flynn, *Icarus* **77**, 287 (1989)
- K. Fredriksson, R. Gowdy, *Geochim. Cosmochim. Acta* **27**, 241 (1963)
- R. Ganapathy, D.E. Brownlee, P. Hodge, *Science* **201**, 1119 (1983)
- M.J. Genge, M.M. Grady, *Meteorit. Planet. Sci.* **33**, 425 (1998)
- M.J. Genge, M.M. Grady, *Lunar Planet. Sci. Conf.* **33**, #1010 (2002)
- M.J. Genge, C. Engrand, M. Gounelle, S. Taylor, *Meteorit. Planet. Sci.* **43**, 497 (2008)
- R.P. Harvey, N.W. Dunbar, W.C. McIntosh, R.P. Esser, K. Nishiizumi, S. Taylor, M.W. Caffee, *Geology* **26**, 607 (1998)
- A. Hashimoto, M. Kumazawa, M. Onuma, *Earth Planet. Sci. Lett.* **43**, 13 (1979)
- A. Hashimoto, *Geochem. J.* **17**, 111 (1983)
- G.F. Herzog, S. Xue, G.S. Hall, L.E. Nyquist, C.-Y. Shih, H. Wiesmann, D.E. Brownlee, *Geochim. Cosmochim. Acta* **63**, 1443 (1999)
- E. Jarosewich, J.A. Nelen, J.A. Norberg, *Geostand. Newsl.* **4**, 257 (1980)
- C. Jehanno, D. Broclet, Ph. Bonte, A. Castellarin, R. Rocchia, *Lunar Planet. Sci. Conf.* **18**, 623 (1988)
- C. Koeberl, E.H. Hagen, *Geochim. Cosmochim. Acta* **53**, 937 (1989)
- A.N. Krot, K. Keil, C.S. Goodrich, E.R.D. Scott, M.K. Weisbert, in *Meteorites, Comets and Planets. Treatise on Geochemistry*, vol. 1, ed. by A.M. Davis (Elsevier Pergamon, Amsterdam, 2005), p. 83
- G. Kurat, C. Koeberl, T. Presper, F. Brandstatter, M. Maurette, *Geochim. Cosmochim. Acta* **58**, 3879 (1994)
- F.T. Kyte, *Analyses of Extraterrestrial Materials in Terrestrial Sediments*. Ph.D. Thesis, University of California, Los Angeles, 1983, pp. 152
- T. Laevastu, O. Mellis, *Trans. AGU* **36**, 385 (1955)
- S.G. Love, D.E. Brownlee, *Science* **262**, 550 (1993)
- U.B. Marvin, M.T. Einaudi, *Geochim. Cosmochim. Acta* **31**, 1871 (1967)
- M. Maurette, C. Hammer, D.E. Brownlee, N. Reeh, H.H. Thomsen, *Science* **233**, 869 (1986)
- M. Maurette, C. Jehanno, E. Robin, C. Hammer, *Nature* **328**, 699 (1987)
- M. Maurette, C. Olinger, M. Christophe Michel-Levy, G. Kurat, M. Purchet, M. Brandstatter, M. Bourot-Denise, *Nature* **351**, 44 (1991)
- H.T. Millard, R.B. Finkleman, *J. Geophys. Res.* **75**, 2125 (1970)
- J. Murray, A.F. Renard, *Proc. R. Soc. Edinb.* **12**, 474 (1883)
- J. Murray, A.F. Renard, A report on the scientific results of the voyage of HMS Challenger during the years 1873–76. *Deep Sea Depos.* 327–336 (1891)
- M.T. Murrell, P.A. Davis, K. Nishiizumi, H.T. Millard, *Geochim. Cosmochim. Acta* **44**, 2067 (1980)
- K. Nishiizumi, J.R. Arnold, D.E. Brownlee, M.W. Caffee, R.C. Finkel, R.P. Harvey, *Meteoritics* **30**, 728 (1995)
- K. Parashar, M.S. Prasad, *Lunar Planet. Sci. Conf.* **XXXIX**, 1045 (2008)
- H. Pettersson, K. Fredriksson, *Pac. Sci.* **12**, 71–81 (1958)

- B. Peucker-Ehrenbrink, in *Accretion of Extraterrestrial Matter Throughout Earth's History*, ed. by B. Peucker-Ehrenbrink, B. Schmitz (Kluwer, New York, 2001), p. 163
- M.S. Prasad, M. Sudhakar, *Meteorit. Planet. Sci.* **34**, 179 (1999)
- M.S. Prasad, S.M. Gupta, V.N. Kodagali, *Meteorit. Planet. Sci.* **38**, 1373 (2003)
- E. Robin, M. Christophe, M. Bourot-Denise, C. Jehanno, *Earth Planet. Sci. Lett.* **97**, 181 (1990)
- P. Rochette, L. Folco, C. Suavet, M. van Ginneken, J. Gattacceca, N. Perchiazzi, R. Braucher, R. Harvey, Micrometeorites from the transantarctic mountains. *Proc. Natl. Acad. Sci. USA* **105**, 18206–18211 (2008)
- A.E. Rubin, *Meteorit. Planet. Sci.* **32**, 231 (1997)
- N.G. Rudraswami, K. Parashar, M.S. Prasad, *Meteorit. Planet. Sci.* (2010) (manuscript submitted)
- B. Schmitz, M. Tassinari, B. Peucker-Ehrenbrink, *Earth Planet. Sci. Lett.* **194**, 1 (2001)
- B. Schmitz, T. Haggstrom, *Meteorit. Planet. Sci.* **41**, 455 (2006)
- R. Tagle, J. Berlin, *Meteorit. Planet. Sci.* **43**, 541 (2008)
- S. Taylor, D.E. Brownlee, *Meteoritics* **26**, 203 (1991)
- S. Taylor, J.H. Lever, R.P. Harvey, *Meteorit. Planet. Sci.* **35**, 651 (2000)
- S. Taylor, J.H. Lever, in *Accretion of Extraterrestrial Matter Throughout Earth's History*, ed. by S. Peucker-Ehrenbrink, B. Schmitz (Kluwer, New York, 2001), p. 205
- S. Taylor, G.F. Herzog, J.S. Delaney, *Meteorit. Planet. Sci.* **42**, 223 (2007)
- J.T. Wasson, G.W. Kallemeyn, *Philos. Trans. R. Soc. Lond. A* **325**, 535 (1988)
- F. Wlotzka, *Meteorit. Planet. Sci.* **40**, 1673 (2005)